第38卷第9期
2022年9月

无 机 化 学 学 报
CHINESE JOURNAL OF INORGANIC CHEMISTRY

Vol.38 No.9
1853-1861

一种带吡啶悬臂大环异双核Zn(Ⅱ)-Ni(Ⅱ)配合物的合成、晶体结构及其DNA结合/切割性质

丁佩佩[1] 李 铭[2] 吴 宇[2] 闫俊涛[1] 王春蕾[1] 王 洋[1] 毛佳伟*,[2]

([1]武汉轻工大学化学与环境工程学院,武汉 430023)

([2]成都市产品质量监督检验所,成都 610100)

摘要: 合成了一种带吡啶悬臂的不对称大环异双核金属Zn(Ⅱ)-Ni(Ⅱ)配合物[ZnNi(L)]$(ClO_4)_2\cdot H_2O$(H_2L=3,3′-((ethane-1,2-diylbis((pyridin-2-ylmethyl)azanediyl))bis(methyl ene)) bis(2-hydroxy-5-methylbenzaldehyde)),通过红外光谱、电喷雾质谱、单晶X射线衍射对其结构进行了表征。结果表明Zn(Ⅱ)和Ni(Ⅱ)的配位环境分别为扭曲的三角锥和正四面体。利用紫外光谱、粘度实验和循环伏安法对该配合物与DNA的相互作用模式进行了研究,结果表明配合物与小牛胸腺DNA(CT-DNA)的结合方式为插入模式,其相应的结合常数K_b=1.05×10^5 L·mol^{-1}。另外,该配合物对pBR322 DNA有一定的切割作用。

关键词: 悬臂大环配合物; 晶体结构; 配位环境; DNA结合; DNA切割

中图分类号: O614.24$^+$1; O614.81$^+$3 **文献标识码:** A **文章编号:** 1001-4861(2022)09-1853-09

DOI: 10.11862/CJIC.2022.199

Synthesis, Crystal Structure, and DNA Binding/Cleavage Properties of a Macrocyclic Heterobinuclear Zn(Ⅱ)-Ni(Ⅱ) Complex with Pyridylmethyl Pendant-Arms

DING Pei-Pei[1] LI Ming[2] WU Yu[2] YAN Jun-Tao[1] WANG Chun-Lei[1] WANG Yang[1] MAO Jia-Wei*,[2]

([1]*School of Chemical and Environmental Engineering, Wuhan Polytechnic University, Wuhan* 430023, *China*)

([2]*Institute of Product Quality Supervision and Inspection, Chengdu* 610100, *China*)

Abstract: A bis-pyridine pendant-armed macrocyclic heterobinuclear Zn(Ⅱ)-Ni(Ⅱ) complex [ZnNi(L)]$(ClO_4)_2\cdot H_2O$ (H_2L=3,3′-((ethane-1,2-diylbis((pyridin-2-ylmethyl)azanediyl))bis(methylene)) bis(2-hydroxy-5-methylbenzaldehyde)) has been obtained and characterized by spectroscopy, elemental analysis and single-crystal X-ray diffraction. The coordination environment of Zn(Ⅱ) and Ni(Ⅱ) can be described as approximately distorted triangular prism and square pyramid, respectively. The Zn—Ni distance bridged by two phenoxide groups is 0.303 63(6) nm. The interaction between the complex and calf thymus DNA (CT-DNA) has been further confirmed by UV-Vis spectrophotometry, viscosity, and cyclic voltammetry study. The complex showed a good binding property to CT-DNA with a binding constant of 1.05×10^5 L·mol^{-1}. The DNA cleavage activity has also been investigated using agarose gel electrophoresis. CCDC: 2045334.

Keywords: pendant-armed macrocyclic complex; crystal structure; coordination environment; DNA binding; DNA cleavage

收稿日期:2022-03-21。收修改稿日期:2022-08-01。

湖北省重点研发项目(No.2020BBB068)和湖北省自然基金(No.2020CFB400)资助。

*通信联系人。E-mail:wyydcc@163.com

0 Introduction

It has been studied that DNA is the primary intracellular target of many cancer drugs because the interaction between complexes and DNA can induce DNA damage in cancer cells, and inhibit the division of aggressive growing cells leading to cell death[1-3]. As the most important step for DNA activity, the binding interaction of transition metal complexes with DNA has been extensively explored[4-5]. To design effective anticancer drugs, the choice of metal ion and the environment of the ligand which dominates the DNA-binding and cleavage ability are the key factors. The Zn(Ⅱ) ion has the potential to influence many aspects of cellular signally through its effect on Zn-binding proteins because there are many transcription facts and enzymes containing Zn-binding sites[6]. Macrocyclic Schiff-base complexes with the Ni(Ⅱ) ions have great application in DNA binding and are used as cleavage agents[7].

Recently, the macrocycles bearing pendant arms and their metal complexes have received considerable attention, because the functionalized pendant arms can provide additional donors, enhance the stability of complexes and allow for modification of the environment of the ligand[8-9]. Haines et al. studied the methylnaphthalene pendant providing steric bulk around the macrocycle[10]. Furfural pendant arms attached to the macrocyclic complex were reported with the binding constant on the order of 10^4[11]. Pan et al. synthesized thiophenoethyl pendant armed macrocyclic complexes whose pendant arms do not coordinate with the metal ions and result in the highly twisted saddle-form configurations matching with the double-helical DNA[12].

In previous work, we reported an unsymmetrical phenyl pendant-armed macrocyclic with heterobinuclear Cu(Ⅱ)-Ni(Ⅱ) complex[13], which showed good phosphate hydrolysis and DNA binding illustrating that the rigid aromatic ring in the macrocycle ligand may have a synergistic effect in DNA. To further clarify the influence of pendant arms in the complex during the DNA binding process, we prepared a new Zn(Ⅱ)-Ni(Ⅱ) heterobinuclear macrocyclic complex bearing two pyridyl pendant arms (Scheme 1). The binding property and cleavage activity of the complex to calf thymus DNA (CT-DNA) have been investigated through UV-Vis spectrophotometry and agarose gel electrophoresis.

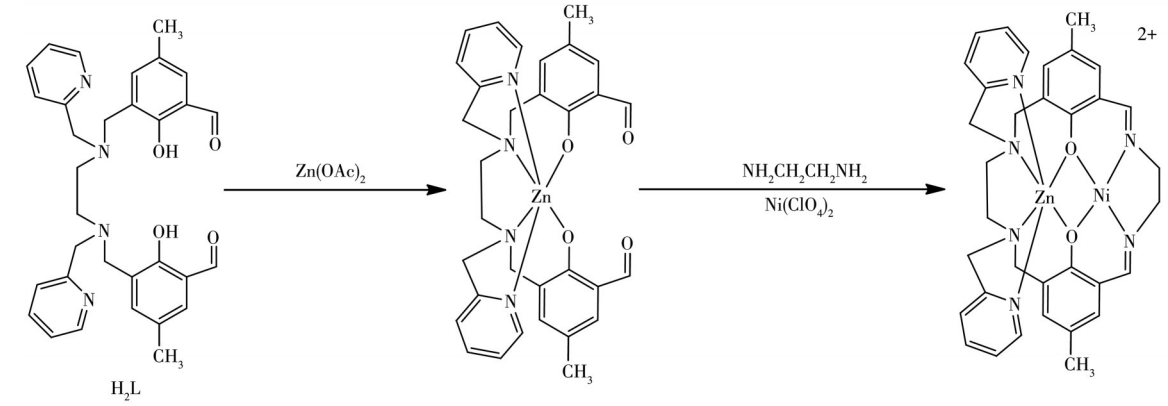

Scheme 1 Synthetic route for the preparation of the Zn(Ⅱ)-Ni(Ⅱ) complex

1 Experimental

1.1 Materials and instruments

The chemicals such as paraformaldehyde, hydrobromic acid, 2-methyl pyridine, 5-methylbenzaldehyde, and triethylamine were of analytical grade obtained from commercial sources. The solvents, namely methanol, ethanol, and *N*, *N*-dimethylformamide (DMF), were purified according to the literature[14]. Tetra(*n*-butyl) ammonium perchlorate (TBAP) was redistilled three times and then dried in a vacuum before use. CT-DNA was supplied by Sigma. The supercoiled pBR322 DNA, trimethylammonium (Tris), agarose gel, and bromophenol blue were purchased from Toyobo Co.

IR spectra were measured on an FT-IR spectrome-

ter with samples prepared as KBr disk. The contents of carbon, hydrogen, and nitrogen element were determined on a Perkin - Elmer 240c element automatic analyzer. UV - Vis spectra were run on a Shimadzu UV-2450 spectrophotometer in a range of 200-700 nm using a cuvette of 1 cm path length. ES - MS spectra were recorded on a Finnigan LCQ ES-MS mass spectrograph using acetonitrile as the mobile phase with an approximate concentration of 1.0 mmol·L^{-1}.

1.2 Synthesis of the complex

The ligand 3,3′-((ethane-1,2-diylbis((pyridin-2-ylmethyl)azanediyl))bis(methylene)) bis(2-hydroxy-5-methylbenzaldehyde) (H_2L) was synthesized according to the literature[15]. A solution of $Zn(OAc)_2·2H_2O$ (0.055 g, 0.25 mmol) in absolute ethanol (10 mL) was added dropwise to an solution (10 mL) of H_2L (0.55 g, 0.25 mmol) in anhydrous ethanol. The mixture was stirred for 2 h at room temperature, then the ethanol solution (10 mL) of ethylenediamine (0.015 g, 0.25 mmol) was added slowly. The resulting green soluting was stirred for 4 h, then the Ni(Ⅱ) perchlorate hexahydrate (0.091 g, 0.25 mmol) dissolved in 10 mL anhydrous methanol was added slowly. The mixture was stirred for 5 h resulting in a red solution. After filtration, the solution was evaporated for three weeks at ambient temperature, and red diamond single crystals of $[ZnNi(L)](ClO_4)_2·H_2O$ suitable for X - ray diffraction analysis were obtained. Yield: 0.131 g (58%). Anal. Calcd. for $C_{68}H_{76}Cl_4N_{12}Ni_2O_{22}Zn_2$(%): C, 45.29; H, 4.25; N, 9.32. Found(%): C, 45.35; H, 4.21; N, 9.42.

1.3 Determination of the crystal structure

The crystal structure of the complex was measured on a Bruker Smart Apex-Ⅱ CCD diffractometer at 173.15 K using graphite monochromatic Mo $K\alpha$ radiation (λ=0.071 073 nm). Data reduction and cell refinement were performed by the SAINT program. The structure was obtained by direct methods (SHELXS) and refined on F^2 by full-matrix least-squares (SHELXS) using all unique data. The non-hydrogen atoms were refined with anisotropic displacement parameters. All hydrogen atoms in the structure were located in calculated positions and refined using riding constraints. The summary of the crystallographic data is listed in Table 1.

CCDC: 2045334.

Table 1 Crystal data and structure refinement for the complex

Parameter	Complex	Parameter	Complex
Empirical formula	$C_{68}H_{76}Cl_4N_{12}Ni_2O_{22}Zn_2$	D_c / (g·cm^{-3})	1.563
Formula weight	1 803.37	μ (Mo $K\alpha$) / mm^{-1}	1.323
Space group	$P\bar{1}$	F(000)	1 856
a / nm	1.276 95(9)	Crystal size / mm	0.20×0.23×0.26
b / nm	1.699 28(11)	θ range / (°)	1.1-26.0
c / nm	1.995 39(13)	N_{ref}, N_{par}	15 051, 1 019
α / (°)	76.819(1)	Total and unique reflection (R_{int})	28 463, 15 051 (0.046)
β / (°)	74.140(2)	Observed data [$I>2\sigma(I)$]	12 458
γ / (°)	68.357(1)	R_1, wR_2, S	0.049 4, 0.108 2, 1.114
Volume / nm^3	3.831 9(4)	Maximum and average shift / error	0.000 and 0.000
Z	2	$(\Delta\rho)_{max}$, $(\Delta\rho)_{min}$ / (e·nm^{-3})	320, −890

1.4 DNA binding experiments

All the experiments involving the interaction of the complexes with DNA were carried out in Tris-HCl buffer (100 mL, 50 mmol·L^{-1} Tris-HCl, 50 mmol·L^{-1} NaCl, pH=7.2) kept at 0 ℃ for less than 4 d.

Absorption spectral studies. CT-DNA (20 mg) was dissolved in Tris-HCl buffer. The ratio of UV absorbance at 260 and 280 nm was in a range of 1.8-2.0 indicating that CT-DNA was free from protein[16]. The concentration of CT-DNA in terms of nucleotide was calculated from its absorption intensity at 260 nm with a molar extinction coefficient of 6 600 L·mol^{-1}·cm^{-1}[17]. The complex was dissolved in DMF at a concentration of 50 μmol·L^{-1}. The UV absorption titration

experiments were performed by keeping the complex concentration constant and varying the CT-DNA concentration. The complex-DNA solution was incubated for 30 min at room temperature before measurements were taken. The binding ability of the complex was calculated by the intrinsic binding constant K_b according to Eq.**1**[18]:

$$c_{DNA}/(\varepsilon_a-\varepsilon_f)=c_{DNA}/(\varepsilon_b-\varepsilon_f)+1/[K_b(\varepsilon_b-\varepsilon_f)] \quad (1)$$

Where c_{DNA} is the concentration of DNA; ε_a, ε_f, and ε_b are the molar extinction coefficient of solutions containing both complex and DNA, free complex, and the complex fully binding to DNA, respectively. When we take $c_{DNA}/(\varepsilon_a-\varepsilon_f)$ as the ordinate and c_{DNA} as the abscissa to draw the graph, the slope of the plot gives the value of $1/(\varepsilon_b-\varepsilon_f)$, while the intercept is equal to $1/[K_b(\varepsilon_b-\varepsilon_f)]$.

Electrochemical studies. The cyclic voltammetric technique is useful for probing the mode of the binding of metal complexes to DNA. Electrochemical measurements were carried out on a CHI 750 electrochemical analyzer with a three-electrode cell system with a glassy carbon as the working electrode, a platinum wire as the counter electrode, and an Ag/AgCl electrode as the reference electrode. The scanning rates were in a range of 20-200 mV·s^{-1}. The solution was deoxygenated by purging with a nitrogen atmosphere before measurements.

Viscosity measurements. Viscosity measurement was performed using a capillary viscometer in a thermostatic water bath maintained at 25 ℃. Flow times were recorded with a digital stopwatch. Each sample was measured three times.

1.5 DNA cleavage experiment

The cleavage of plasmid DNA by the complex was monitored using agarose gel electrophoresis. A mixture of Tris-HCl buffer, pBR322 DNA (0.25 μg·μL^{-1}), and different amounts of the complexes (dissolved in DMF) was incubated for 3 h at 37 ℃. The reaction in the samples was quenched by the addition of sterile solution (1 μL, 0.25% bromophenol blue solution, 0.4 g·mL^{-1} sucrose solution). The samples were then analyzed by electrophoresis for 0.8 h at 100 V in TAE buffer (40 mmol·L^{-1} Tris, 20 mmol·L^{-1} acetic acid, and 1 mmol·L^{-1} EDTA, pH=7.4). The gel was stained with ethidium bromide (EB, 1 μg·μL^{-1}) for 0.5 h after electrophoresis and then photographed.

2 Results and discussion

2.1 Synthesis and characterization

The synthetic route for the preparation of the Zn(Ⅱ)-Ni(Ⅱ) complex is depicted in Scheme 1. In the IR spectrum of the complex, the appearance of sharp stretching vibration at 1 617 cm^{-1} ($\nu_{C=N}$) and the absence of the stretching vibrations between 1 740 and 1 720 cm^{-1} ($\nu_{C=O}$) confirm the formation of the Schiff base macrocyclic framework and the aldehyde groups has been completely converted into imine groups[19]. A strong intensity band at 1 090 cm^{-1} and one medium intensity band at 624 cm^{-1} correspond to ν_3 and ν_4 absorptions of perchlorate ions. The sharp instead of broad peak at 1 090 cm^{-1} assigns that the perchlorate ions are not coordinated to the metal ions and are present as counter ions in the crystal lattice, which was in agreement with the crystal structure[20]. Further, the appearance of a band in the region of 1 550-1 571 cm^{-1} refers to the phenolate bridging with the metal ions[21]. The complex exhibited a band centered between 3 400 and 3 500 cm^{-1} originating from ν_{O-H} of water present. Although in absence of structural information, the IR data might be useful in determining the coordination geometry of metal in the [N_4O_2] coordination site.

The ES-MS spectrum of the complex was measured in acetonitrile solution (Supporting information). The dominant molecular ion peaks appear at *m/z* 743.33 corresponding to the solvation species [ZnNi(L)(C_2H_3N)(H_2O)]$^{2+}$, where the complex lost two ClO_4^-, and break into two same units. And the peaks that appeared at *m/z* 342.33 are attributed to the ligand H_2L. This chromatographic behavior suggests that perchlorate ion dissociated from [ZnNi(L)](ClO_4)$_2$. The other observed peaks may be assigned to various fragments arising from the thermal cleavage of the complex.

2.2 Crystal structure of [ZnNi(L)](ClO_4)$_2$·H_2O

The perspective view of [ZnNi(L)]$^{2+}$ and the metal coordination environment polyhedron are given in Fig.1. Selected bond lengths and angles relevant to the Zn(Ⅱ) and Ni(Ⅱ) coordination spheres of the complex

are listed in Table 2. The heterobinuclear Zn(Ⅱ)-Ni(Ⅱ) complex consists of two $[ZnNi(L)]^{2+}$ cations, four ClO_4^- anions as counter ions, and two water molecules, the corresponding formula is $[ZnNi(L)]_2(ClO_4)_4 \cdot (H_2O)_2$. The complex contains two similar macrocyclic units (Fig. 1, A and B), and each unit is just like a butterfly waving its wings. The two pyridine pendant arms play the roles of wings which are situated in the same sidepiece of the mean molecular plane.

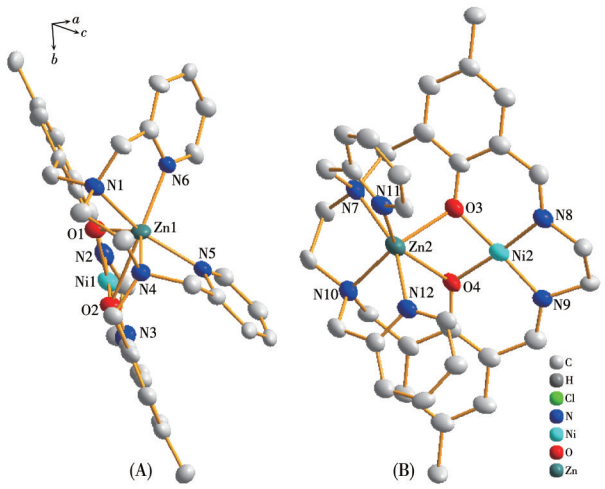

Fig.1 Perspective view of $[ZnNi(L)]^{2+}$ at 30% probability thermal ellipsoids with hydrogen atoms omitted for clarity

Each unit of the complex shows that the Zn(Ⅱ) center coordinated with four nitrogen donors and two phenoxide atoms to yield an overall metal coordination geometry of six while the Ni(Ⅱ) ion resides at the $[N(imine)_2O_2]$ site in four coordinated compartments with a square plane topology. The coordination geometry of Zn(Ⅱ) can be described as a distorted trigonal prism. The Ni(Ⅱ) ion with a d^8 electronic configuration tends to form four-coordinated planar complexes[15]. The bond distances around the Zn(Ⅱ) ion are in a range of 0.203 1(3)-0.243 6(3) nm, which are comparable with those reported in other similar heterobinuclear complexes[20-21], and longer than the mononuclear and homobinuclear complex[22-23]. The basal bond distances around the Ni(Ⅱ) ion range from 0.184 2(3) to 0.186 3(3) nm, which are shorter than the homobinuclear complex[24]. The Zn—Ni distance bridged by two phenolic oxygens is 0.303 63(6) nm, which is an effective metal-

Table 2 Selected bond distances (nm) and angles (°) for complex

Zn1—O1	0.206 1(3)	Zn2—O4	0.239 4(2)	Ni1—N2	0.184 0(3)
Zn1—O2	0.243 4(2)	Zn2—N7	0.216 9(3)	Ni1—N3	0.184 8(3)
Zn1—N1	0.215 2(3)	Zn2—N10	0.215 5(3)	Ni2—O3	0.181 7(3)
Zn1—N4	0.216 7(3)	Zn2—N11	0.211 4(3)	Ni2—O4	0.182 9(2)
Zn1—N5	0.209 6(3)	Zn2—N12	0.211 6(3)	Ni2—N8	0.185 3(3)
Zn1—N6	0.213 0(3)	Ni1—O1	0.181 6(2)	Ni2—N9	0.182 8(3)
Zn2—O3	0.205 2(2)	Ni1—O2	0.182 4(2)		
O2—Ni1—O1	80.39(10)	N5—Zn1—N6	97.66(11)	O3—Zn2—N11	91.45(10)
O2—Ni1—N3	96.25(12)	O2—Zn1—N1	118.82(10)	N12—Zn2—N11	95.94(11)
O1—Ni1—N3	175.27(13)	N5—Zn1—N1	153.67(12)	O3—Zn2—N7	87.32(11)
O1—Ni1—N2	95.90(12)	N6—Zn1—N1	77.90(11)	N12—Zn2—N7	157.51(11)
O2—Ni1—N2	176.20(12)	O2—Zn1—N4	80.23(9)	N11—Zn2—N7	79.87(11)
N3—Ni1—N2	87.50(14)	N5—Zn1—N4	80.18(11)	O3—Zn2—N10	136.55(11)
O4—Ni2—O3	80.64(11)	N6—Zn1—N4	132.58(11)	N12—Zn2—N10	80.68(11)
O3—Ni2—N9	177.38(12)	N1—Zn1—N4	83.99(11)	N11—Zn2—N10	128.68(11)
O4—Ni2—N9	96.79(12)	O2—Zn1—O1	62.37(9)	N7—Zn2—N10	84.81(11)
O4—Ni2—N8	174.68(12)	N5—Zn1—O1	116.86(11)	O3—Zn2—O4	63.57(9)
O3—Ni2—N8	94.38(12)	N6—Zn1—O1	90.96(10)	N12—Zn2—O4	78.91(10)
N9—Ni2—N8	88.17(13)	N1—Zn1—O1	89.31(10)	N11—Zn2—O4	148.06(11)
O2—Zn1—N5	79.05(10)	N4—Zn1—O1	132.55(10)	N7—Zn2—O4	116.03(10)
O2—Zn1—N6	146.43(10)	O3—Zn2—N12	114.98(11)	N10—Zn2—O4	82.0(1)

metal distance for phosphomonoesterase mimics[9]. The Zn(Ⅱ) ions lie out of the approximate [N(amine)$_2$O$_2$] planar by 0.096 83 nm in A and 0.095 39 nm in B, and Ni(Ⅱ) ions lie almost on the [N(imine)$_2$O$_2$] plane for A and B with the deviation of −0.001 99 and −0.001 90 nm, respectively, which indicates the Zn(Ⅱ) and Ni(Ⅱ) are in the opposite side of the planar. The dihedral angle between the [N(amine)$_2$O$_2$] and [N(imine)$_2$O$_2$] planes is 18.092(71)°. The average distances of Zn1 and Zn2 to the 18-member macrocyclic ring are 0.152 9 and 0.153 2 nm, which are longer than the literature reported before[25]. It may be decided by the number of carbon atoms related to imine nitrogen atoms. The fewer carbon atoms lead to smaller microcycles ring size and shorter bond distances between metal atoms and coordinating atoms, then Zn^{2+} lies more away from the macrocyclic ring.

2.3 DNA-binding activity

2.3.1 Absorption spectral studies

Electronic absorption spectroscopy is universally used to determine the binding characteristics of a metal complex with DNA. The absorption spectra of the complex in the absence and presence of increasing amounts of CT-DNA (0-75 μmol·L^{-1}) are shown in Fig.2. In general, hypochromicity and redshift are considered evidence of the intercalative mode of binding between the aromatic chromophore of the complex and the base pairs of DNA[26]. In the UV region, the mixture of complex and CT-DNA showed a big hypochromism (15%) at the band of 380 nm with a small amount of red-shift (2 nm) at a ratio of $c_{DNA}/c_{complex}$ of 3. The moderate change observed in the absorption spectra indicates that the binding of complex to DNA double-helix is an intercalative mode[27]. The mechanism could explain the hypochromism and red-shift: after the complex intercalates the base pairs of DNA through diffusion, the π-orbital of the base pairs couple with the π^*-orbital of the intercalated ligand, thus decreasing the π-π^* transition energy and resulting the red-shift. At the same time, electrons partially fill the coupling π^*-orbital and then decrease the probabilities of transition resulting in hypochromism.

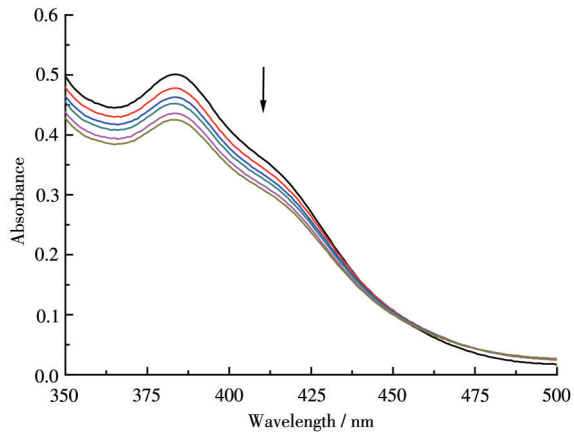

Arrow shows the absorbance changes upon increasing the DNA concentrations

Fig.2 Absorption spectra of the Zn(Ⅱ)-Ni(Ⅱ) complex in the absence and presence of increasing amounts of CT-DNA (0-75 μmol·L^{-1}) at 25 ℃ in 50 mmol·L^{-1} Tris-HCl/NaCl (pH=7.2)

The intrinsic binding constant K_b was calculated from the ratio of slope to intercept of the plot of $c_{DNA}/(\varepsilon_a-\varepsilon_f)$ vs c_{DNA} (Fig. 3) and found to be 1.05×10^5 L·mol^{-1}. Hence, the binding affinity of the complex is higher than the previously reported symmetric heterobinuclear Zn(Ⅱ)-Ni(Ⅱ) complex[28]. We can deduce that the Zn(Ⅱ)-Ni(Ⅱ) complex binds to DNA by intercalation. The pyridyl nitrogen took part in the coordination, which leads to the distorted pyridyl ring plane, and the methyl electron-donating effect on the benzene ring resulted in the decrease of the planar rigidity, then lead to moderate intercalation.

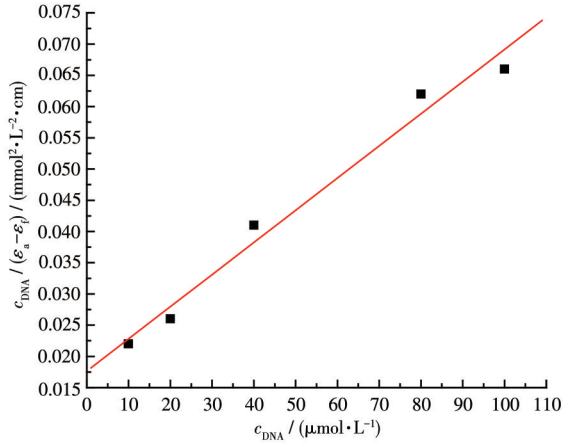

Fig.3 Plot of $c_{DNA}/(\varepsilon_a-\varepsilon_f)$ vs c_{DNA} for UV-Vis absorption titration of the complex with CT-DNA

2.3.2 Electrochemical study

To further prove the complex intercalation to DNA, the electrochemical properties of the complex were studied by cyclic voltammetry in 50 mmol·L^{-1} Tris-HCl/50 mmol·L^{-1} NaCl buffer solution (pH=7.2) using TBAP as supporting electrolytes in a sweeping range of −1.4 to −0.4 V at room temperature. It was delineated that the cathodic and anodic peak potential both shifted toward negative or positive value, which means the intercalation of the complex into the base pairs of the DNA, while the different shift means the grooving and electrostatic interaction of the complex with DNA[29]. The cyclic voltammogram of the complex (0.5 mmol·L^{-1}) in the absence and presence of CT-DNA is shown in Fig. 4. In the absence of CT-DNA, the cathodic peak potential (E_{pc}) and the anodic peak potential (E_{pa}) were −0.832 and −0.689 V, respectively. The separation (ΔE) of the anodic and cathodic peak potentials was 0.143 V which was bigger than 0.059 V, suggesting a pseudo-reversible electrochemical process. The addition of CT-DNA to the complex resulted in a decrease in the cathodic and anodic peak currents and both peak potentials shifted to bigger values with E_{pc}=−0.815 V and E_{pa}=−0.607 V. The reduction in peak current intensity and positive shift in potential in the presence of CT-DNA is due to the intercalation binding of this complex with CT-DNA[11]. By comparison, in the reported cyclic voltammogram of heterobinuclear Zn(Ⅱ)-Ni(Ⅱ) complex[30], irreversible redox processes were observed with E_{pc}=−1.58 V. The behavior was similar to the reported complexes with diamino propane lateral chains instead of the diaminoethane chain in this complex[28].

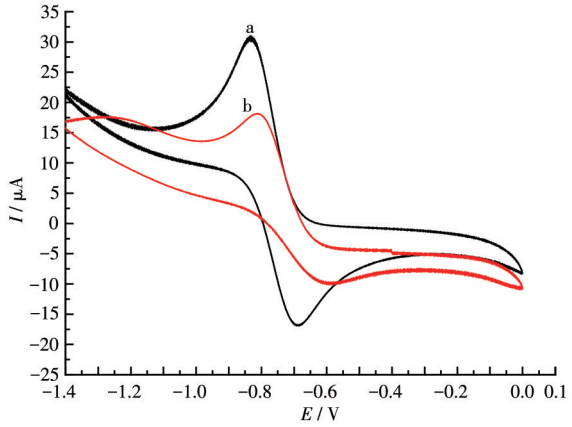

Fig.4 Cyclic voltammogram of the complex in the absence (a) and presence (b) of CT-DNA

2.3.3 Viscosity titration

Viscosity measurement is regarded as the most critical test in evaluating the binding interactions of the complex with DNA due to that the viscosity of DNA is sensitive to its length[31]. A classical intercalation model leads to the CT-DNA helix lengthening as base pairs are separated to accommodate the binding ligand, which results in the viscosity enhancement, while the grooving and electrostatic binding would exert no such effect on the viscosity[32]. As shown in Fig. 5, with the increasing amount of the complex, the relative viscosity of DNA increased steadily, which indicates that the complex bind to DNA through intercalation mode. This result is according to the absorption spectroscopy and cyclic voltammogram studies.

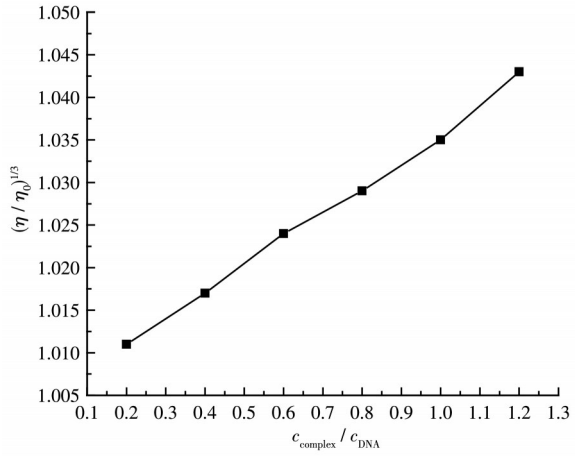

c_{DNA}=0.2 mmol·L^{-1}

Fig.5 Effect of increasing amounts of the complex on the relative viscosity of DNA

2.4 DNA cleavage activity

The supercoiled pBR322 DNA cleavage ability has been investigated with various concentrations of the complex by agarose gel electrophoresis experiment since the synthesized complex satisfies one of the primary criteria for catalyzing hydrolytic cleavage of DNA, *i.e.* coordination of the phosphate moiety of DNA to the metal center of complex[25]. The cleavage efficacy of the complex is shown in Fig. 6. This complex could transform Form Ⅰ (supercoil form) to Form Ⅱ (open

circular form) at 200 μmol·L^{-1}. No linear coil form was found indicating that the complex was involved in single-strand breaking. Compared with other macrocyclic complexes, the DNA cleavage activity of this complex[24] was lower for it cleaved SC DNA to NC DNA in higher concentration. This may be due to the pyridyl N taking part in the coordination and destroying the planarity of the complex.

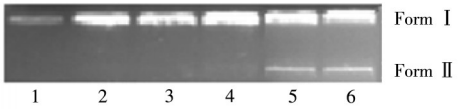

Lane 1: DNA control; Lane 2-6: DNA + the complex (25, 50, 100, 200, 400 μmol·L^{-1}, respectively); Incubation time: 3 h

Fig.6 Agarose gel electrophoresis of pBR322 plasmid DNA in the presence of different concentrations of the complex

3 Conclusions

This work involved the synthesis and structurally characterization of a new bis-pyridine pendant-armed macrocyclic heterbinuclear Zn(Ⅱ)-Ni(Ⅱ) complex. The studies of UV-Vis absorption, viscosity, and cyclic voltammetry of the mixture of the complex and DNA showed high binding capacity. The binding ability is affected by the substituents in the ligand and the size of the ring cavity. Compared with the K_b value, the complex has a moderate stronger binding than some reported similar complexes. Moreover, this heterobinuclear complex showed an efficient cleavage activity toward pBR322 DNA in the absence of any external agents.

Supporting information is available at http://www.wjhxxb.cn

References:

[1]Rad F V, Housaindokht M R, Jalal R, Hosseini H E, Doghaei A V, Goghari S S. Spectroscopic and Molecular Modeling Based Approaches to Study on the Binding Behavior of DNA with a Copper(Ⅱ) Complex. *J. Fluoresc.*, **2014**,**24**:1225-1234

[2]Navarro M, Cisneros-Fajardo E J, Sierralta A, Fernández-Mestre M, Silva P, Arrieche D, Marchán E. Design of Copper DNA Intercalators with Leishmanicidal Activity. *J. Biol. Inorg. Chem.*, **2003**,**8**:401-408

[3]Ljubijankic N, Zahirovic A, Turkusic E, Kahrovic E. DNA Binding Properties of Two Ruthenium(Ⅲ) Complexes Containing Schiff Bases Derived from Salicylaldehyde: Spectroscopic and Electrochemical Evidence of CT DNA Intercalation. *Croat. Chem. Acta*, **2013**,**86**:215-222

[4]Shahabadi N, Kashanian S, Darabi F. DNA Binding and DNA Cleavage Studies of a Water Soluble Cobalt(Ⅱ) Complex Containing Dinitrogen Schiff Base Ligand: The Effect of Metal on the Mode of Binding. *Eur. J. Med. Chem.*, **2010**,**45**:4239-4245

[5]Aldulmani S A A. Spectral, Modeling, DNA Binding/Cleavage and Biological Activity Studies on the Newly Synthesized 4-[(Furan-2-ylmethylene)amino]-3-[(2-hydroxy-benzylidene) amino]-phenyl-methanone and Some Bivalent Metal(Ⅱ) Chelates. *J. Mol. Struct.*, **2021**,**1226**:129356

[6]Asayama S, Nishinohara S, Kawakami H. Zinc-Chelated Poly(1-vinylimidazole) and a Carbohydrate Ligand Polycation Form DNA Ternary Complexes for Gene Delivery. *Bioconjugate Chem.*, **2011**, **22**: 1864-1868

[7]Jullian V, Sheperd E, Gelbrich T, Hursthouse M B, Kilbrun J D. New Macrobicyclic Receptors for Amino Acids. *Tetrahedron Lett.*, **2000**,**20**(41):3963-3966

[8]Hirohama T, Arii H, Chikira M. EPR Study of the Dynamic Behavior of *cis*,*cis*-1,3,5-Triaminocyclohexane Cu(Ⅱ) Complex on B-Form DNA-Fibers. *J. Inorg. Biochem.*, **2004**,**98**:1778-1786

[9]Anbu S, Kandaswamy M, Varghese B. Structural, Electrochemical, Phosphate-Hydrolysis, DNA Binding and Cleavage Studies of New Macrocyclic Binuclear Nickel(Ⅱ) Complexes. *Dalton Trans.*, **2010**,**39**:3823-3832

[10]Hanies R I, Hutchings D R. Synthesis and X-ray Crystal Structure of *meso*-5,5,7,12,12,14-Hexamethyl-1,4,8,11-tetraazacyclotetradecane-1,8-di-(1-methylnaphthalene). *Molecules*, **2003**,**8**:243-250

[11]Kumar A, Vashistha V K, Tevatia P, Singh R. Electrochemical Studies of DNA Interaction and Antimicrobial Activities of Mn^{Ⅱ}, Fe^{Ⅲ}, Co^{Ⅱ} and Ni^{Ⅱ} Schiff Base Tetraazamacrocyclic Complexes. *Spectroc. Acta Pt. A-Molec. Biomolec. Spectr.*, **2017**,**26**:123-133

[12]Pan Z Q, Ding K, Zhou H, Cheng R Q, Chen Y F, Huang Q M. Syntheses, Structures and Properties of Dinickel(Ⅱ) Macrocyclic Complexes with Two 2-Thiophenoethyl Pendant Arms. *Polyhedron*, **2011**, **30**:2268-2274

[13]Ding P P, Wang Y, Kou H Z, Li J F, Shi B X. Synthesis of Heterobinuclear Cu(Ⅱ)-Ni(Ⅱ) Complex: Structure, CT-DNA Interaction, Hydrolytic Function and Antibacterial Studies. *J. Mol. Struct.*, **2019**,**1196**:836-843

[14]Wang Y, W Xia, Mao J W, Zhou H, Pan Z Q. Phosphate Ester Hydrolysis and DNA Binding Capacity of Two New Dinuclear Ni(Ⅱ) Complexes. *J. Mol. Struct.*, **2013**,**1036**:361-371

[15]Prabu R, Vijayaraj A, Suresh R, Shenbhagaraman R, Kaviyarasan V, Narayanan V. Electrochemical, Catalytic and Antimicrobial Activity of N-Functionalized Tetraazamacrocyclic Binuclear Nickel(Ⅱ) Complexes. *Spectroc. Acta Pt. A-Molec. Biomolec. Spectr.*, **2011**,**78**:601-606

[16]Lachkar M, Guilard R, Attamani A, Cian A D, Fischer J, Weiss R. Synthesis of New Binucleating Cylindrical Macrotricyclic Ligands where Two Cyclam Rings are in a Face-to-Face Conformation. Char-

acterization of Their Dicopper(Ⅱ) and Dinickel(Ⅱ) Complexes. *Inorg. Chem.*, **1998**,**37**(7):1575-1584

[17]Golchoubian H, Mardani H R, Bruno G, Rudbari H A. Effect of Alkyl Group on the Structure of Heterodinuclear Zn(Ⅱ)-Cu(Ⅱ) and Zn(Ⅱ)-Ni(Ⅱ) Complexes Derived from Unsymmetrical Phenol-Based Dicompartmental Macro-Acyclic Ligands. *J. Iran. Chem. Soc.*, **2013**, **10**:29-41

[18]Wolfe A, Shimer G H, Meehan T. Polycyclic Aromatic Hydrocarbons Physically Intercalate into Duplex Regions of Denatured DNA. *Biochemistry*, **1987**,**26**:6392-6393

[19]Rao C R K, Zacharias P S. Studies of Dinuclear Metal Complexes of Macrocyclic Ligands. *Polyhedron*, **1997**,**16**:1201-1209

[20]Golchoubian H, Baktash E, Welter R. Synthesis and Characterization of Mono- and Hetero- Dinuclear Complexes with Dicompartmental Macrocyclic Ligand Containing Hexa- and Pentadentate Coordination Sites. *Inorg. Chem. Commun.*, **2007**,**10**:120-124

[21]Golchoubian H, Mardani H R, Bruno G, Rudbari H A. Synthesis of Mono and Heterodinuclear Complexes with Unsymmetrical Phenol-Based Dicompartmental Ligand Containing Hexa and Tetradentate Coordination Sites: An Unusual Methyl Elimination in Coordination Chemistry. *Inorg. Chem. Acta*, **2012**,**383**:250-256

[22]Saghatforoush L, Moeini K, Hosseini-Yazdi S A, Mardani Z, Bakhtiari A, Hajabbas-Farshchi A, Honarvar S, Abdelbaky M S M. Effective Anticancer Activities of an Acyclic Symmetrical Compartmental Schiff Base Ligand and Its Co(Ⅱ), Cu(Ⅱ) and Zn(Ⅱ) Complexes Against the Human Leukemia Cell Line K562. *Polyhedron*, **2019**,**170** (15):312-324

[23]Kou H Z, Wang Y, Ding P P, Cheng X Z, Zhou G W. Synthesis, Crystal Structure, Phosphate Hydrolysis Activity and Antibacterial Activity of Macrocyclic Dinuclear Zn(Ⅱ) Complex with Benzyl Pendant-Arms. *J. Mol. Struct.*, **2020**,**1216**:128299

[24]丁超, 陈云峰, 刘明, 宋会婷, 周红, 潘志权. 不对称大环双核Ni(Ⅱ)配合物的DNA切割性能研究. 无机化学学报, **2002**,**4**(28):801-808

DING C, CHEN Y F, LIU M, SONG H T, ZHOU H, PAN Z Q. Studies on an Unsymmetrical Macrocyclic Dinuclear Ni(Ⅱ) complex Interaction with DNA. *Chinese J. Inorg. Chem.*, **2002**,**4**(28):801-808

[25]Aidi M, Keypour H, Shooshtari A, Bayat M, Hosseinzadeh L, Rudbari H A, Gable R W. Coordination Chemistry of Some New Mn(Ⅱ), Cd(Ⅱ) and Zn(Ⅱ) Macrocyclic Schiff Base Complexes Containing a Homopiperazine Head Unit. Spectral, X-ray Crystal Structural, Theoretical Studies and Anticancer Activity. *Inorg. Chim. Acta*, **2019**,**490**:294-302

[26]Fei B L, Xu W S, Tao H W, Li W, Zhang Y, Long J Y, Liu B Q, Xia B, Sun W Y. Effects of Copper Ions on DNA Binding and Cytotoxic Activity of a Chiral Salicylidene Schiff Base. *J. Photochem. Photobiol. B*, **2014**,**132**(5):36-44

[27]Chao H, Mei W J, Huang Q W, Ji L N. DNA Binding Studies of Ruthenium(Ⅱ) Complexes Containing Asymmetric Tridentate Ligands. *J. Inorg. Biochem.*, **2002**,**92**:165-170

[28]Mao J W, Zhou H, Chen Y F, Cheng G Z, Pan Z Q. Synthesis, Structure, DNA Interaction, and Hydrolytic Function toward Bis(*p*-nitrophenyl) Phosphate of a Heterobinuclear Macrocyclic Complex. *Transition Met. Chem.*, **2012**,**37**:385-391

[29]Sakthivel A, Raman N, Mitu L. DNA Interaction Studies of Pyrazolone- and Diimine-Incorporated Mn(Ⅱ), Co(Ⅱ), Ni(Ⅱ), Cu(Ⅱ), and Zn(Ⅱ) Complexes: Synthesis, Spectroscopic Characterization, and Antimicrobial Study. *Monatsh. Chem.*, **2013**,**144**:605-620

[30]Parimala S, Kandaswamy M. Mononuclear, Dinuclear Nickel(Ⅱ) and Heterodinuclear Zn(Ⅱ)Ni(Ⅱ) Complexes as Models for the Active Site of Phosphatase. *Inorg. Chem. Commun.*, **2003**,**6**(9):1252-1254

[31]Gurumoorthy P, Mahendiran D, Prabhu D, Arulvase C, Rahiman A K. Mixed-Ligand Copper(Ⅱ) Phenolate Complexes: Synthesis, Spectral Characterization, Phosphate-Hydrolysis, Antioxidant, DNA Interaction and Cytotoxic Studies. *J. Mol. Struct.*, **2015**,**1080**:88-98

[32]Anbu S, Kandaswamy M, Kamalraj S, Muthumarry J, Varghese B. Phosphatase-like Activity, DNA Binding, DNA Hydrolysis, Anticancer and Lactate Dehydrogenase Inhibition Activity Promoting by a New Bis-phenanthroline Dicopper(Ⅱ) Complex. *Dalton Trans.*, **2011**, **40**:7310-7318